

Poly(vinylidene fluoride)/Silica Nanocomposite Membranes by Electrospinning

Xi Xiong, Qiang Li, Xu-Cheng Zhang, Li Wang, Zhao-Xia Guo, Jian Yu

Department of Chemical Engineering, Key Laboratory of Advanced Materials (MOE), Tsinghua University, Beijing 100084, People's Republic of China

Correspondence to: J. Yu (E-mail: yujian03@mail.tsinghua.edu.cn)

ABSTRACT: Poly(vinylidene fluoride) (PVDF)/silica nanocomposite membranes containing up to 30% silica were prepared by electrospinning using colloidal silica as the source of silica and dimethyl formamide as the solvent. The fiber morphology was observed by field emission scanning electron microscopy. The average fiber diameter is about 0.3 μm for PVDF/silica composite fibers having 10–30% silica. Silica nanoparticles were observed on all fiber surfaces with fairly good dispersion and distribution. Fourier transform infrared spectroscopy and differential scanning calorimeter were used to investigate the crystallization behavior of PVDF and showed that a mixture of α -, β -, and γ -phase crystals was obtained with little content of α phase and all the PVDF/silica composite membranes have similar degree of crystallinity. Static water contact angle measurements were performed to investigate the surface wettability of the membranes. The mechanical properties were evaluated by tensile tests, showing strong reinforcement effect. The tensile modulus and tensile strength increase significantly when silica is present. © 2012 Wiley Periodicals, Inc. *J. Appl. Polym. Sci.* 129: 1089–1095, 2013

KEYWORDS: electrospinning; mechanical properties; crystallization; composites

Received 25 June 2012; accepted 30 October 2012; published online 23 November 2012

DOI: 10.1002/app.38787

INTRODUCTION

Poly(vinylidene fluoride) (PVDF) is one of the most important membrane materials. PVDF microporous membranes have been widely used in various fields such as filtration, polymer electrolyte in lithium batteries, and membrane distillation. Commercially, they are produced mainly by phase inversion technique.¹

Electrospinning is a simple and effective processing technique extensively exploited in the last decade for producing ultrafine fibers. The electrospinning products are in the form of membranes having high porosity as a result of random deposition of the fibers. The electrospun nanofibrous membranes have been investigated for various applications including those of traditional membranes such as filtration, showing good performance.^{2,3} They are expected to replace the currently available membranes.⁴ Therefore, the electrospinning of the membrane materials such as PVDF is of high interest. PVDF electrospun membranes have been produced and some applications have been investigated, giving encouraging results.^{5–13} For example, Choi et al.⁵ prepared PVDF membranes by electrospinning from various acetone/dimethyl acetamide-mixed solvent compositions and investigated their application as polymer electrolytes in lithium cells with good electrochemical properties. However, the

mechanical properties of the electrospun membranes are usually weak.

Polymer/inorganic nanocomposites usually have better mechanical properties than the corresponding neat polymers. Nano-sized silica is one of the commonly used reinforcing nanofillers. It has been found that nanosilica can improve significantly the mechanical properties of polyimide,¹⁴ PVDF,^{15–17} and thermoplastic polyurethane (TPU)¹⁸ electrospun membranes. PVDF/silica electrospun nanofibrous membranes have been prepared by two approaches in view of the way of silica introduction. One is electrospinning blend solutions of PVDF and a precursor of silica (tetraethyl orthosilicate or tetramethyl orthosilicate) and generating silica after electrospinning by thermal treatment.^{16,17} The other is incorporating silica powder into PVDF solution and producing PVDF/silica composite membranes by coelectrospinning.¹⁵ In both approaches, nanosilica loading is limited, because a large amount of silica precursor incorporated into the electrospinning solution will significantly decrease the solution viscosity, and a big addition of silica powder to the electrospinning solution will cause severe dispersion problem, resulting in unsuccessful electrospinning.

In our previous study,^{18,19} PMMA/silica and TPU/silica nanocomposite fibers were successfully prepared by coelectrospinning PMMA and TPU with nanosilica using colloidal silica as the source of silica, and we found that the silica loading can be varied in a wide range up to 30 wt % (relative to the polymer) with good dispersion. In this study, PVDF/silica nanocomposite fibers are prepared in a similar way. The silica loading is varied between 0 and 30 wt % to investigate the effects of silica loading on the fiber morphology, crystallization behavior, wettability, and mechanical properties of the composite membranes.

EXPERIMENTAL

Materials

PVDF (Solef 9009) with melt mass flow rate of 7.0–13 g/10 min (230°C, 3.8 kg) was produced by Solvay Specialty Polymers, New Jersey, USA. Tetraethyl orthosilicate (TEOS) of 98% purity was purchased from Sigma-Aldrich. Dimethyl formamide (DMF) and concentrated ammonia (25–28%) were purchased from Beijing Chemical, Beijing, China. Ethanol was purchased from Beijing Tongguang Fine Chemical, Beijing, China. All the chemicals were used without further purification.

Preparation of Colloidal Silica Using Sol–Gel Method

The colloidal silica was prepared according to the previously published literature procedure.²⁰ In brief, 160 mL of ethanol, 6 mL of deionized water, and 6 mL of concentrated ammonia were added to a 500-mL round-bottomed flask and heated to 40°C. Six milliliter of TEOS was added. After stirring for 3 h, another 4 mL of TEOS was added. After 3 h, 10 mL of DMF was added. Then, ethanol, water, and ammonia were removed by a rotary evaporator, and colloidal silica in DMF was obtained, which is also called silica sol.

Preparation of Electrospun PVDF/Silica Composite Fibers

The solutions for electrospinning were prepared by stirring PVDF and silica sol in DMF at 60°C for 12 h. The PVDF concentration is 27 wt % for the preparation of composite fibers. The silica concentrations are 10, 20, and 30 wt % relative to PVDF. Electrospinning process was conducted at 35–40°C. The solution was placed into a 10-mL syringe capped with a 9# blunt end needle. The positive lead from a high-voltage supply was connected via an alligator clip to the external surface of needle. A rectangular aluminum foil was bundled around a grounded metal rotary drum (diameter, 8 cm, rotating rate, 400 rpm), which was placed 15 cm from the tip of the needle as a rotating collector. The voltage was kept at 20 kV, and the solution flow rate was 1 mL/125 min. All the samples were dried in a vacuum oven at 60°C for 24 h before testing.

Characterization

The morphology of the fibers was examined using a JSM-7401 field emission scanning electron microscopy (FESEM) apparatus at an accelerating voltage of 1 kV. The average fiber diameters were determined by measuring and averaging the diameter of 50 fibers using JEOL software (SMILEVIEW). To investigate the distribution of silicon on the fibrous membrane, the spectrum of EDX was applied on a JSM-6301 FESEM with an oxford EDS accessory. The porosity was calculated by comparing the actual density and apparent density of a membrane. The apparent

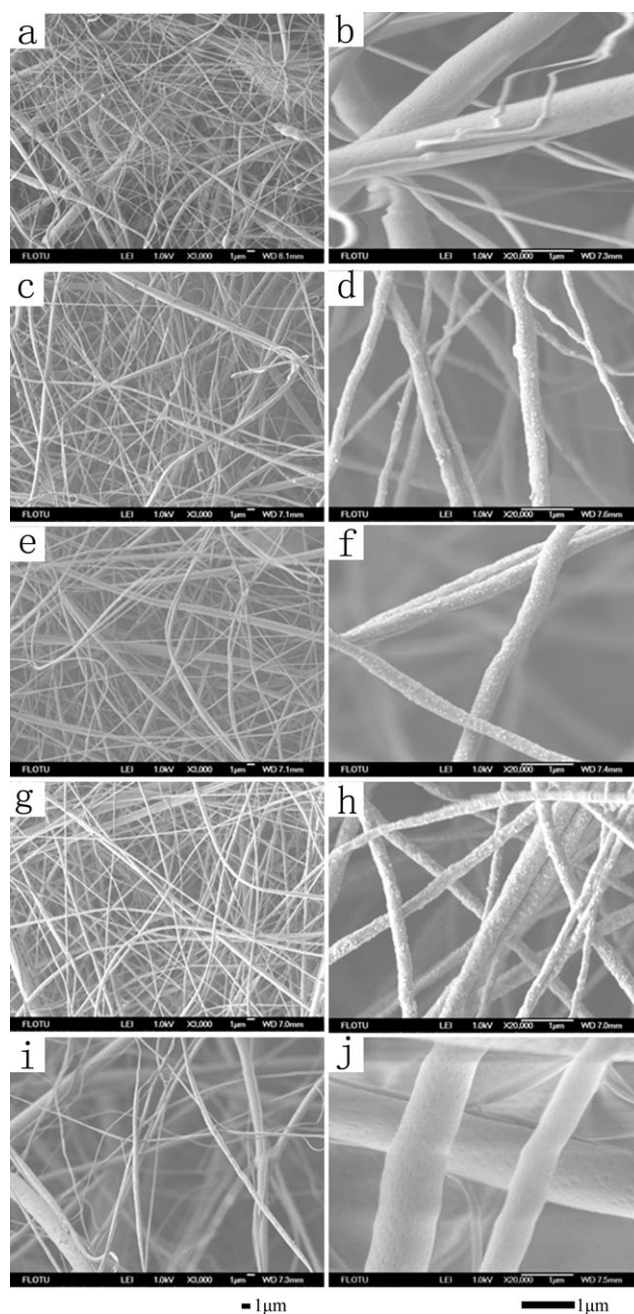


Figure 1. FESEM images of neat PVDF electrospun fibers with electrospinning solution concentration of (a,b) 27% and (i,j) 33%, and PVDF/silica fibers with different silica loadings at PVDF concentration of 27% (c,d) 10%, (e,f) 20%, (g,h) 30%. The magnifications of the images are 3000 \times (left), and 20,000 \times (right).

density was obtained by weighing a precise volume of a membrane. Fourier transform infrared spectroscopy (FTIR) spectra of the fibrous membranes were obtained with a Fourier-transform spectrophotometer (Nicolet, MAGNA-IR 560) by averaging 32 scans at a resolution of 4 cm^{-1} in the range of 4000–450 cm^{-1} . Transmission electron microscopy (TEM) image was taken using a JEM 2010 electron microscope (Japan). Particle size, size distribution, and polydispersity index of the

Table I. Thermal Properties, Crystallinities, Porosities, and Static Contact Angles of PVDF/Silica Membranes With Different Silica Loadings

Membrane	Solution conductivity ^a (μS/cm)	Average fiber diameter (μm)	Melting temperature (°C)	Melting enthalpy (J/g)	Crystallinity (%)	Porosity (%)	Contact angle (°)
PVDF	4.5	1.07 ± 0.68	159.2	54.5	52.1	81	134.3 ± 0.6
PVDF/10%SiO ₂	12.9	0.31 ± 0.14	158.4	45.6	43.6	82	126.7 ± 0.3
PVDF/20%SiO ₂	16.6	0.31 ± 0.13	159.0	44.6	42.6	83	115.0 ± 0.4
PVDF/30%SiO ₂	22.1	0.36 ± 0.05	159.3	43.6	41.7	82	125.9 ± 0.9

^aMeasured at 40°C.

silica nanoparticles were determined by a ZETAPARTICLE HS3000 Laser particle size and ζ-potential analyzer. Differential scanning calorimeter (DSC) was carried out on a Q100 calorimeter (TA Instruments, USA) at a heating rate of 10°C/min under a constant stream of nitrogen. The degree of crystallinity was calculated using a standard melting enthalpy of 104.6 J/g^{21,22} assuming the same value for all the crystalline forms of PVDF. The water contact angles were measured with a sessile drop method using a Dataphysics OCA-20 contact angle analyzer, the droplet volume was 4 μL. Tensile tests were performed on a TCS-2000 tensile tester (Gotech) at an extension rate of 5 mm/min with and rectangular-shaped samples (50 × 10 mm²).

RESULTS AND DISCUSSION

Electrospinning of PVDF/Silica Composite Solutions

As the major component of composite fibers, the concentration of the polymer is an important parameter affecting fiber morphology. Therefore, suitable PVDF concentration was investigated prior to the change of silica loading by electrospinning PVDF/20%SiO₂ composite solutions with different PVDF concentrations. When PVDF concentration was 27%, almost smooth fibers were obtained (Figure 1). When PVDF concentration increases to 29%, the solution viscosity became very high and the solution was gel-like, difficult to electrospin. When

PVDF concentration decreased to 25%, beads-on-string structure was obtained with spherical beads up to 8.5 μm in diameter. Thus, PVDF concentration of 27% was chosen for investigating the effect of silica loading.

As shown in Figure 1, when neat 27% PVDF was electrospun, there were many beads, some of which were very big. Macroscopically, the electrospun membrane contains grains, indicating the occurrence of electrospray along with electrospinning. However, almost smooth fibers were obtained with all the composite solutions regardless of silica loading. This can be understood by the increases in solution viscosity which can be observed visually and conductivity (Table I) after the incorporation of silica,¹⁹ resulting in improved electrospinnability.²³ The average fiber diameters are 0.31, 0.31, and 0.36 μm for fibers containing 10, 20, and 30% of silica, respectively. No much change in fiber diameter was observed when silica loading increased, because the increases in solution viscosity and conductivity show opposite effects on fiber diameter. It is commonly known that the increase in solution viscosity increases fiber diameter, whereas the increase in conductivity decreases fiber diameter.^{24,25}

For neat PVDF, almost smooth fibers can be obtained only when the concentration increases to 33% (Figure 1), where the solution viscosity is visually much higher than that of 27% PVDF solution. The fiber diameter has a wide distribution with an average value of 1.07 μm, much larger than those of PVDF/silica composite fibers. All the discussion in the next sections uses this sample as the control representing neat PVDF fibers.

At big magnification (20,000×), silica nanoparticles were observed on FESEM photos of the fibers [Figure 1(d,f,h)]. when silica loading is low (10%), most silica nanoparticles are monodisperse with a size of about 35 nm, and randomly arranged on fiber surface. When silica loading increased, more silica nanoparticles were observed on fiber surface and the average interparticle distance decreases. With 30% silica, silica nanoparticles have a fairly homogeneous distribution although slight accumulation occurs. The good dispersion and distribution of silica nanoparticles suggest the existence of the interaction between the PVDF chains and the silanol groups of silica,^{18,19,26} which is confirmed by the shift of C—F stretching peak from 1174 to 1182 cm⁻¹ in FTIR spectra (Figure 2).

Distribution of Silica Nanoparticles in PVDF/Silica Fibers

The size and dispersion of the silica nanoparticles in silica sol were characterized by TEM and laser particle analyzer. Figure

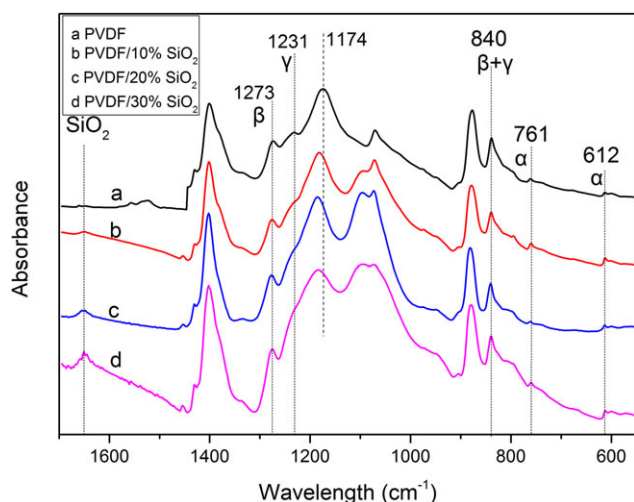


Figure 2. FTIR spectra of the electrospun PVDF/silica membranes. [Color figure can be viewed in the online issue, which is available at www.interscience.wiley.com.]

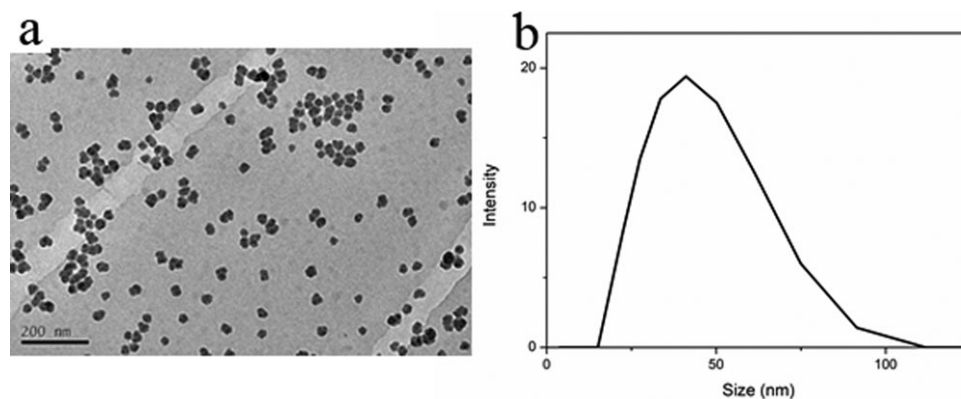


Figure 3. Colloidal silica nanoparticles: (a) TEM photograph and (b) particle size distribution measured by laser scattering.

3(a) shows the TEM image of the colloidal silica nanoparticles, indicating monodispersity and almost no agglomeration of the nanoparticles. The mean particle diameter shown in the TEM micrograph is 33 nm. The particle size distribution characterized by laser particle analyzer is shown in Figure 3(b), showing a mean diameter of 37 nm and polydispersity index of 0.138, further confirming the monodispersity of silica nanoparticles.

The distributions of silica nanoparticles on the surfaces of PVDF/silica fibrous membranes are investigated by EDX. As shown in Figure 4, EDX spectra indicate the presence of silica on the external surfaces of all the composite membranes. The silicon and oxygen peaks appear after incorporation of silica. EDX Si-mapping micrographs of the fiber mats are shown in Figure 5. The bright spots representing the silicon element (figures on the right side) indicate a homogeneous distribution of silicon (thus silica nanoparticles) in all the fiber mats containing silica.

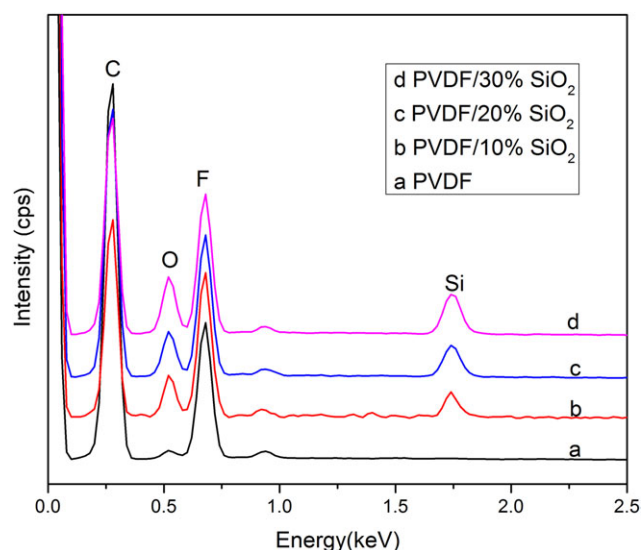


Figure 4. EDX spectra of the PVDF/silica electrospun membranes. [Color figure can be viewed in the online issue, which is available at wileyonlinelibrary.com.]

The dispersion of silica nanoparticles in the composite fibers was observed by TEM. The images are shown in Figure 6. It can be observed that the distribution of silica nanoparticles is fairly homogeneous and with increasing silica content, the particle distribution density increases without obvious agglomeration.

Crystallization Behavior of PVDF

PVDF is known for its polymorphism, and infrared spectroscopy is frequently used to identify and quantify the different PVDF phases.^{6–8,11,27–29} The α phase has vibration bands at 612 and 761 cm^{-1} , and the β phase has vibration bands at 840 and 1273 cm^{-1} , whereas the γ phase shows characteristic peaks at 838 and 1231 cm^{-1} . Figure 2 shows the FTIR spectra of PVDF membranes containing 0, 10, 20, and 30% silica. The α , β , and γ phases are present in all the samples, and the peaks of the α phase at 612 and 761 cm^{-1} have very weak absorption compared to that of the β phase at 1273 cm^{-1} . The peak of the γ phase at 1231 cm^{-1} is obvious in neat PVDF membrane and decreases significantly when silica is present in the sample. The predominance of electroactive β and γ phases is favorable for making electronic devices.

The polymorphism of PVDF electrospun membranes has been extensively investigated.^{8,10,11,27} Some authors¹¹ reported coexistence of α , β , and γ phases and some others^{10,21} reported a mixture of α and β phases with β -phase domination. Zheng et al.¹¹ reported that PVDF electrospun fibers with α -, β -, or γ -phase domination can be fabricated by controlling the electrospinning parameters. Andrew and Clarke¹⁰ showed that electrospinning is a simple one-step procedure to form β -rich PVDF material with up to 75% β phase. Ribeiro et al.²⁷ concluded that all the electrospinning parameters leading to a higher stretching of the jet or straining of the fibrils during collection favor the formation of β phase. The results reported in this study suggest that the β -phase content may also be related to the source of PVDF and the presence of other component.

The melting temperature and degree of crystallinity of PVDF crystals in the membranes containing different amounts of silica were investigated by DSC. The curves are shown in Figure 7. For neat PVDF and PVDF/SiO₂ samples, a broad melting peak was observed at around 159°C.

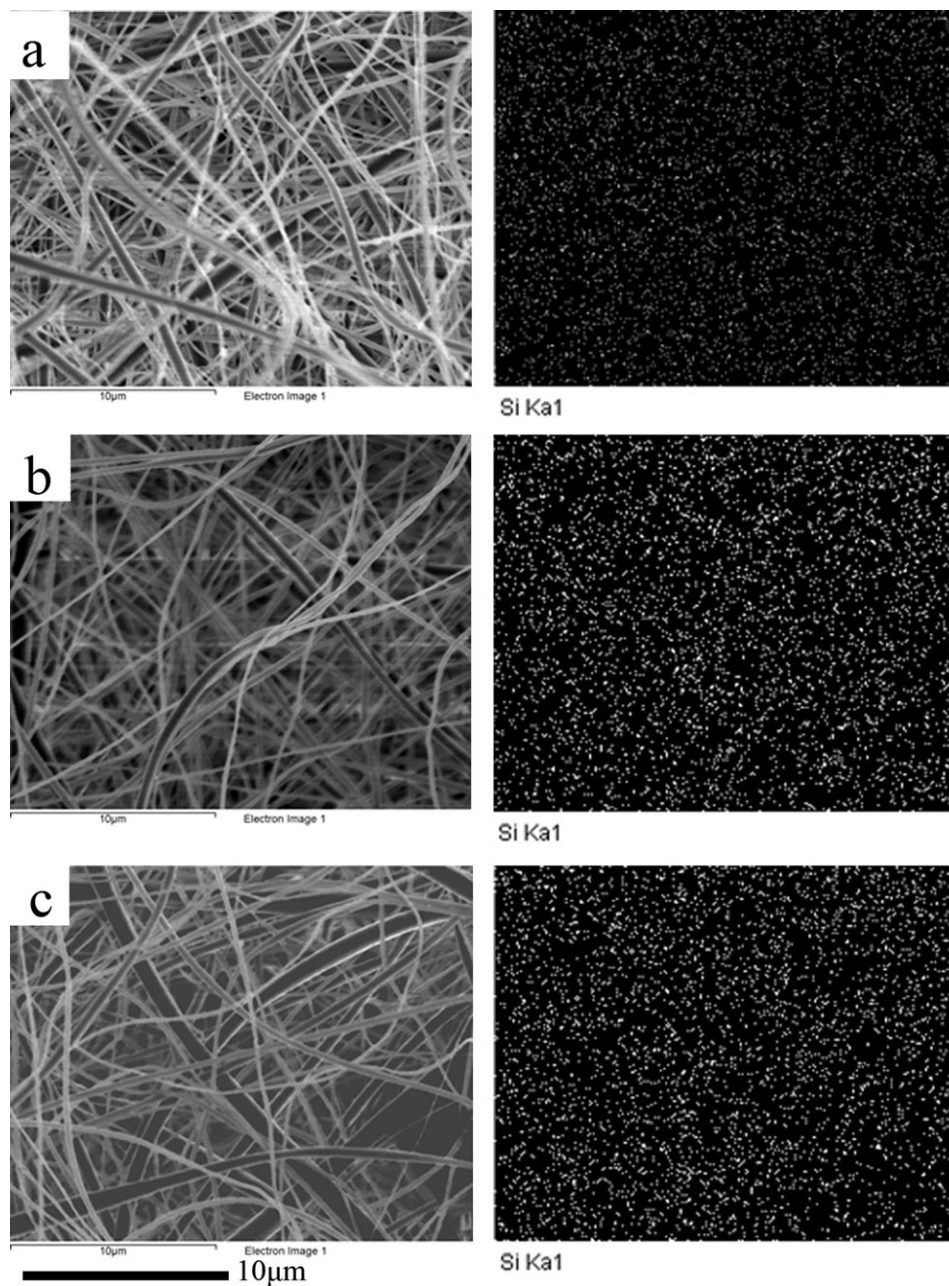


Figure 5. EDX mapping showing Si distribution of PVDF/silica membranes with different silica loadings (a) 10%, (b) 20%, and (c) 30%.

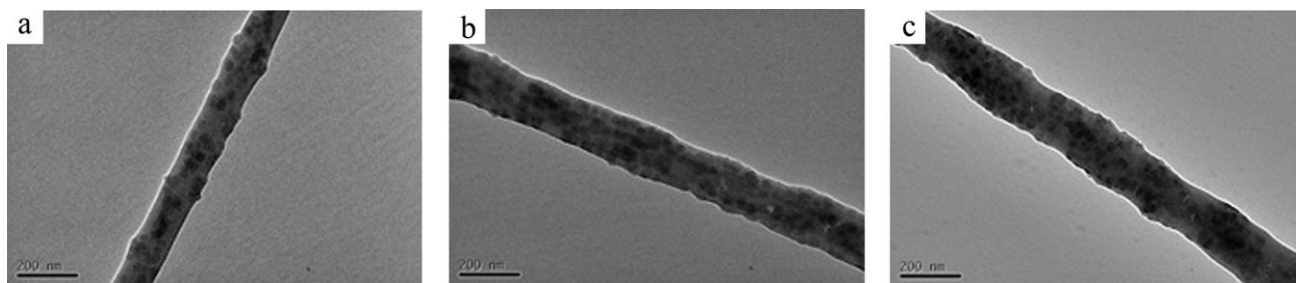


Figure 6. TEM photographs of PVDF/silica electrospun fibers with different silica loadings (a) 10%, (b) 20%, and (c) 30%.

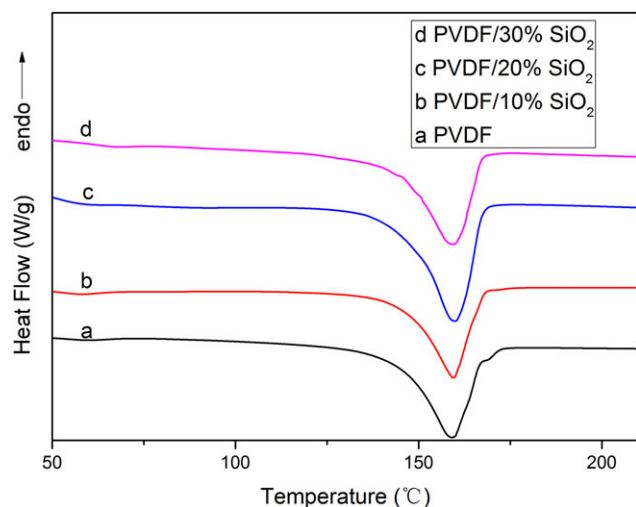


Figure 7. DSC curves of the electrospun PVDF/silica membranes. [Color figure can be viewed in the online issue, which is available at wileyonlinelibrary.com.]

As summarized in Table I, the melting enthalpy of PVDF slightly decreases when silica is present, but almost has no change when silica loading changes. Kim et al.¹⁵ also observed a slight decrease in melting enthalpy after the incorporation of silica in their work dealing with the preparation of electrospun PVDF/silica membranes from silica powder. As the error in the measurement of melting enthalpy is usually big, it can be concluded that the presence of silica does not have significant effect on the degree of crystallinity.

Wettability of PVDF/Silica Membranes

Surface wettability is an important parameter for membranes. Static water contact angle measurements were performed to evaluate the hydrophobicity of the electrospun PVDF/silica membranes containing different amounts of silica, and the results are summarized in Table I. All the PVDF/silica composite membranes have slightly lower contact angles than neat PVDF.

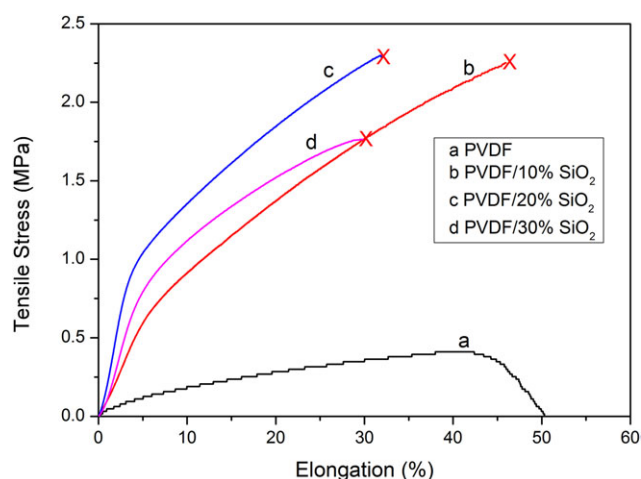


Figure 8. Stress-strain curves of the PVDF/silica electrospun membranes. [Color figure can be viewed in the online issue, which is available at wileyonlinelibrary.com.]

Table II. Mechanical Properties of PVDF/Silica Membranes

Membrane	Modulus (MPa)	Tensile strength (MPa)	Elongation to break (%)
PVDF	1.9 ± 0.4	0.5 ± 0.1	52 ± 2
PVDF/10%SiO ₂	12.0 ± 0.1	2.2 ± 0.1	47 ± 5
PVDF/20%SiO ₂	17.4 ± 1.7	2.1 ± 0.2	35 ± 3
PVDF/30%SiO ₂	10.6 ± 1.2	1.7 ± 0.2	32 ± 1

In general, the surface wettability of the electrospun fibrous membranes is related to a number of factors, not only the hydrophobicity of the membrane material, but also the microstructure of the surface including fiber diameter, the roughness of fiber surface, porosity, pore size, and so on. In this study, the porosity of the PVDF/silica membranes is practically unchanged compared to that of neat PVDF membrane (81–83%), but the fiber diameter is different (0.3 vs. 1.0 μm). The presence of hydrophilic silica on fiber surface decreases the hydrophobicity and increases the surface roughness. Thus, the contact angle value is the result of combined effects of multiple factors. Park et al.¹⁶ found that the water contact angle of PVDF/silica membranes was independent of silica loading and Kim et al.¹⁵ reported a slight change in contact angle for PVDF/silica composite membranes compared to the control PVDF membrane. These along with our results suggest that silica does not have big effect on surface wettability.

Mechanical Properties of PVDF/Silica Membranes

Uniaxial tensile tests were carried out to evaluate the effect of silica on the mechanical properties of PVDF membranes. Typical stress-strain curves are shown in Figure 8, and the average tensile modulus, tensile strength, and elongation to break are summarized in Table II. Compared to neat PVDF membrane, all the PVDF/silica composite membranes have much larger tensile modulus and tensile strength, and slightly lower elongation to break, revealing that silica has a great reinforcing effect. This can be attributed to the good dispersion of silica nanoparticles as seen from FESEM photos and TEM images, and strong hydrogen bonding between PVDF chains bearing electronegative fluorine (F) and the silanol groups of silica, as revealed by the shift of C–F stretching peak from 1174 to 1182 cm⁻¹ in FTIR spectra (Figure 2). The tensile modulus and tensile strengths of PVDF/10%SiO₂ membrane are 6.3 and 4.4 times those of neat PVDF membrane. When silica loading increases to 20%, the tensile modulus increases further to 9.1 times that of neat PVDF membrane, but the tensile strength no longer increases. When silica loading increases further to 30%, both the tensile modulus and the tensile strength decrease owing to presumably the agglomeration of some silica nanoparticles, suggesting that a very large amount of silica is unnecessary for the purpose of reinforcement.

CONCLUSIONS

Electrospun PVDF/SiO₂ composite membranes with good mechanical properties can be prepared with a wide range of silica loading up to 30% using colloidal silica nanoparticles as

the source of silica. When silica loading is 10%, the silica nanoparticles distributed on the fiber surface are monodisperse. More silica nanoparticles were observed on fiber surface with slight accumulation when silica loading increases to 30%. The α -, β -, and γ -phase crystals coexist in PVDF/silica composite membranes with little content of α phase, and the degree of crystallinity does not vary significantly with the change in silica loading. The static water contact angles of PVDF/silica composite membranes are slightly lower than that of neat PVDF membrane. Silica nanoparticles have a strong reinforcing effect. With 10 and 20% silica nanoparticles, the tensile modulus and tensile strength are improved to a great extent, whereas the elongation to break decreases only slightly. The improvement in the mechanical properties can be attributed to the good dispersion of silica nanoparticles and the strong interaction between the PVDF chains and the silanol groups of silica. The method reported in this study can provide a good alternative to the existing approaches for the preparation of electrospun PVDF/silica membranes with the advantages of good silica dispersion and largely variable silica loading.

REFERENCES

1. Bottino, A.; Cameraroda, G.; Capannelli, G.; Munari, S. *J. Membr. Sci.* **1991**, *57*, 1.
2. Huang, Z. M.; Kotaki, M.; Ramakrishna, S. *Compos. Sci. Technol.* **2003**, *63*, 2223.
3. Gopal, R.; Kaur, S.; Ma, Z. W.; Chan, C.; Ramakrishna, S.; Matsuura, T. *J. Membr. Sci.* **2006**, *281*, 581.
4. Cho, E.; Kim, C.; Kook, J. K.; Jeong, Y. I.; Kim, J. H.; Kim, Y. A.; Endo, M.; Hwang, C. H. *J. Membr. Sci.* **2012**, *389*, 349.
5. Choi, S. W.; Kim, J. R.; Ahn, Y. R.; Jo, S. M.; Cairns, E. J. *Chem. Mater.* **2007**, *19*, 104.
6. Crecorio, R., Jr.; Cestari, M. *J. Polym. Sci. Part B: Polym. Phys.* **1994**, *32*, 859.
7. Zhao, Z. Z.; Li, J. Q.; Yuan, X. Y.; Li, X.; Zhang, Y. Y.; Sheng, J. *J. Appl. Polym. Sci.* **2005**, *97*, 466.
8. Yee, W. A.; Kotaki, M.; Liu, Y.; Lu, X. H. *Polymer* **2007**, *48*, 512.
9. Yang, C. R.; Jia, Z. D.; Guan, Z. C.; Wang, L. M. *J. Power Sources* **2009**, *189*, 716.
10. Andrew, J. S.; Clarke, D. R. *Langmuir* **2008**, *24*, 670.
11. Zheng, J. F.; He, A. H.; Li, J. X.; Han, C. C. *Macromol. Rapid Commun.* **2007**, *28*, 2159.
12. Na, H. N.; Zhao, Y. P.; Zhao, C. G.; Zhao, C.; Yuan, X. Y. *Polym. Eng. Sci.* **2008**, *48*, 934.
13. Na, H. N.; Liu, X. W.; Sun, H.; Zhao, Y. H.; Zhao, C.; Yuan, X. Y. *J. Polym. Sci. Part B: Polym. Phys.* **2010**, *48*, 372.
14. Cheng, S.; Shen, D. Z.; Zhu, X. S.; Tian, X. G.; Zhou, D. Y.; Fan, L. J. *Eur. Polym. J.* **2009**, *45*, 2767.
15. Kim, Y. J.; Ahn, C. H.; Lee, M. B.; Choi, M. S. *Mater. Chem. Phys.* **2011**, *127*, 137.
16. Park, S. H.; Lee, S. M.; Han, J. T.; Lee, D. R.; Shin, H. S.; Jeong, Y. J.; Kim, J. Y.; Cho, J. H. *ACS Appl. Mater. Inter.* **2010**, *2*, 658.
17. Kim, Y. J.; Ahn, C. H.; Choi, M. O. *Eur. Polym. J.* **2010**, *46*, 1957.
18. Zhang, X. C.; Chen, Y. Z.; Yu, J.; Guo, Z. X. *J. Polym. Sci. Part B: Polym. Phys.* **2011**, *49*, 1683.
19. Chen, Y. Z.; Zhang, Z. P.; Yu, J.; Guo, Z. X. *J. Polym. Sci. Part B: Polym. Phys.* **2009**, *47*, 1211.
20. Hong, Y. L. Preparation and Characterization of Continuous Long One-dimensional Organic/Inorganic Composite Nanomaterials. PhD Thesis. Jilin: Jilin University, **2005**; Chapter 2, p 38.
21. Rosemberg, Y.; Sigmann, A.; Narkis, M.; Shkolnik, S. *J. Appl. Polym. Sci.* **1991**, *43*, 535.
22. Marega, C.; Marigo, A. *Eur. Polym. J.* **2003**, *39*, 1713.
23. Chen, Y. Z.; Peng, P.; Guo, Z. X.; Yu, J.; Zhan, M. S. *J. Appl. Polym. Sci.* **2010**, *115*, 3687.
24. Tan, S. H.; Inai, R.; Kotaki, M.; Ramakrishna, S. *Polymer* **2005**, *46*, 6128.
25. Huang, Z. M.; Zhang, Y.-Z.; Kotaki, M.; Ramakrishna, S. *Compos. Sci. Technol.* **2003**, *63*, 2223.
26. Song, R.; Yang, D. B.; He, L. H. *J. Mater. Sci.* **2007**, *42*, 8408.
27. Ribeiro, C.; Sencadas, V.; Ribelles, J. L. G.; Lanceros-Mendez, S. *Soft Mater.* **2010**, *8*, 274.
28. Lopes, A. C.; Costa, C. M.; Tavares, C. J.; Neves, I. C.; Lanceros-Mendez, S. *J. Phys. Chem. C* **2011**, *115*, 18076.
29. Ince-Gunduz, B. S.; Alpern, R.; Amare, D.; Crawford, J.; Dolan, B.; Jones, S.; Kobylarz, R.; Reveley, M.; Cebe, P. *Polymer* **2010**, *51*, 1485.